Symmetrical and unsymmetrical dizinc complexes as models for the active sites of hydrolytic enzymes†‡§

Martin Jarenmark,[a] Sascha Kappen,¶[a] Matti Haukka[b] and Ebbe Nordlander*[a]

Received 6th September 2007, Accepted 15th November 2007
First published as an Advance Article on the web 29th November 2007
DOI: 10.1039/b713664a

Dinuclear carboxylate-bridged zinc complexes of one symmetric and one asymmetric phenolate-based ligand catalyse the transesterification of 2-hydroxypropyl-*p*-nitrophenyl phosphate (HPNP) at different rates, with an unsymmetrical complex being more active than a symmetric one.

A plethora of dinuclear metal sites are found in metalloproteins, and dinuclear active sites are found in several classes of metalloenzymes, including monooxygenases (*e.g.* soluble methane monooxygenase,[1,2] tyrosinase[3,4]) and hydrolases[5] (*e.g.* urease[6] and metallo-β-lactamases[7]). In the latter class of enzymes, metal ions with good Lewis acidity and flexible coordination geometry are usually found. Divalent zinc is a typical example of such an ion, and a number of metallohydrolases contain polynuclear metal sites with one or more zinc ions[8,9]; these include leucin aminopeptidase,[10] nuclease P1,[11] kidney bean purple acid phosphatase,[12] alkaline phosphatases[13] and the above-mentioned metallo-β-lactamases.[14] We have shown that symmetrical and unsymmetrical ligands containing terminal carboxylate and methylimidazolyl donor moieties may be used to prepare structural and functional model complexes for dinuclear active sites in metalloenzymes, including hydrolases such as the dinickel enzyme urease and the dizinc enzyme zinc phosphotriesterase.[15–17] Here we wish to describe the synthesis of two new potentially dinucleating ligands, and the preparation of zinc complexes of these ligands that accelerate the hydrolysis/transesterification of the organophosphoester 2-hydroxypropyl-*p*-nitrophenyl phosphate (HPNP).

The trisodium salt of 2,6-bis[*N*-{*N*-(carboxymethyl)-*N*-(pyridylmethyl)amine}methyl]-4-methylphenolate (Na_3BCPMP) and the hexafluorophosphate salt 2-[*N*-isopropyl-*N*-{(2-pyridyl)methyl}-aminomethyl]-6-[*N*-(carboxylmethyl)-*N*-{(2-pyridyl)methyl}-aminomethyl]-4-methylphenol (H_4IPCPMP$(PF_6)_2\cdot H_2O$) could be prepared in 28 and 12% overall yields, respectively, using synthetic methodology explored by Latour and coworkers[18] as well as ourselves[15,16] (Scheme 1). Reaction of a suspension of Na_3BCPMP* in methanol with $Zn(OAc)_2\cdot 2H_2O$ gave the anionic complex $Na_3[Zn_2(BCPMP)(OAc)_2]_2PF_6\cdot 6H_2O$ (**1**).†† The analogous reaction of H_4IPCPMP$(PF_6)_2\cdot H_2O$* with $Zn(OAc)_2$ in a water–methanol mixture, in the presence of three equivalents of sodium methoxide, yielded $[\{Zn_2(IPCPMP)(OAc)\}_2](PF_6)_2$ (**2**).†† Similarly, mixing of H_4IPCPMP$(PF_6)\cdot H_2O$ with $ZnCl_2$ and sodium pivalate in ethanol in the presence of triethylamine yielded $[\{Zn_2(IPCPMP)(O_2CC(CH_3)_3)\}_2](PF_6)_2\cdot H_2O\cdot$EtOH (**3**).†† The structures of complexes **1–3** could be verified by X-ray crystallography.‡‡ The structure of **1** reveals that the complex is C_2-symmetric with the two pyridyl donor moieties *trans* to each other (Fig. 1). The Zn–Zn distance of 3.50 Å is similar to that found in the enzyme zinc phosphotriesterase (3.5 Å)[19] but slightly longer than what is usually found in similar phenolate bridged

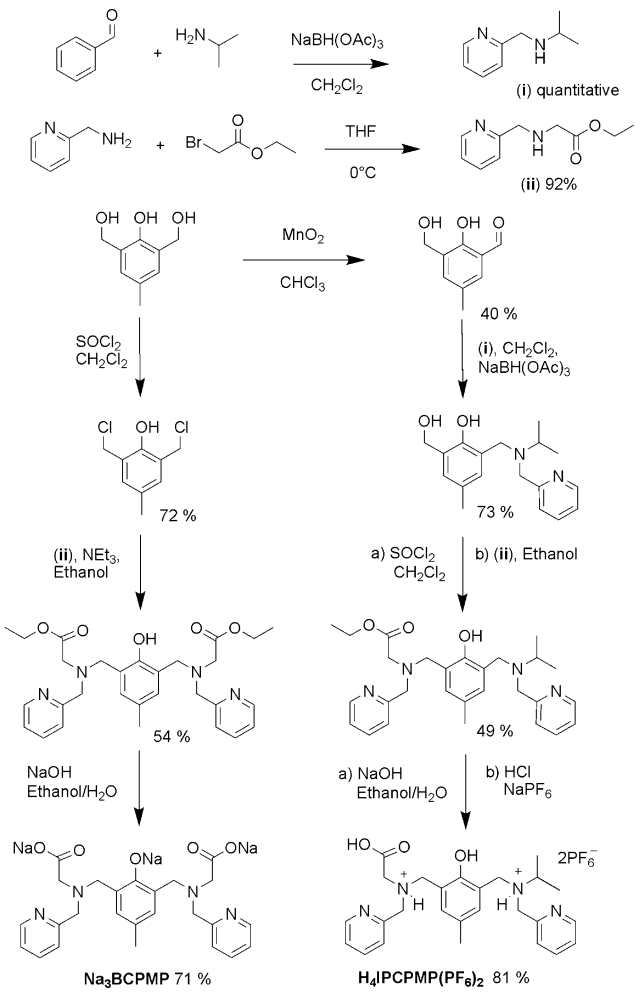

Scheme 1 A schematic depiction of the syntheses of Na_3BCPMP and H_4IPCPMP$(PF_6)_2$.

[a]*Inorganic Chemistry Research Group, Chemical Physics, Center for Chemistry and Chemical Engineering, Lund University, Box 124, SE-221 00 Lund, Sweden. E-mail: Ebbe.Nordlander@chemphys.lu.se; Tel: +46 46 222 8118*
[b]*Department of Chemistry, University of Joensuu, Box 111, FI-80101 Joensuu, Finland*

† The HTML version of this article has been enhanced with colour images.

‡ CCDC reference numbers 659750, 659751, 667079. For crystallographic data in CIF or other electronic format see DOI: 10.1039/b713664a

§ Electronic supplementary information (ESI) available: Fig. S1: an ORTEP representation of the molecular structure of the cation of complex **2**; Fig. S2: FAB mass spectrum of complex **2**; Table S1: crystallographic details for complex **2**. See DOI: 10.1039/b713664a

¶ ERASMUS student from the University of Hamburg, Germany.

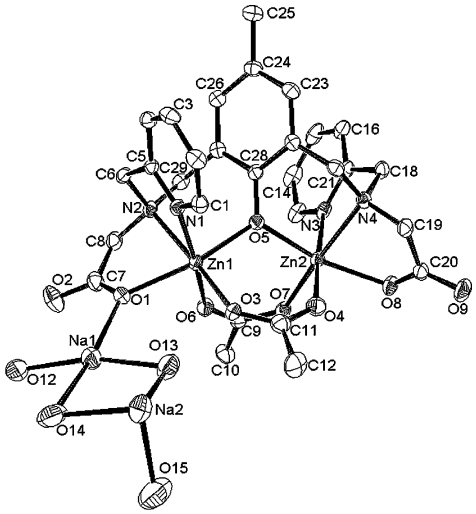

Fig. 1 An ORTEP[29] representation of the structure of **1** showing the atom numbering scheme. Thermal ellipsoids are drawn at the 30% probability level. Hydrogen atoms, non-coordinated counter ions and solvent molecules have been omitted for clarity. Relevant bond distances (Å) and angles (°): Zn(1)–O(5) 2.037(3); Zn(1)–O(3) 2.054(4); Zn(1)–O(6) 2.116(4); Zn(1)–O(1) 2.153(4); Zn(1)–N(1) 2.186(4); Zn(1)–N(2) 2.204(4); Zn(2)–O(5) 2.042(3); Zn(2)–O(7) 2.052(4); Zn(2)–O(4) 2.108(4); Zn(2)–O(8) 2.119(4); Zn(2)–N(3) 2.168(4); Zn(2)–N(4) 2.214(4); Zn(1)–O(5)–Zn(2) 118.07(16).

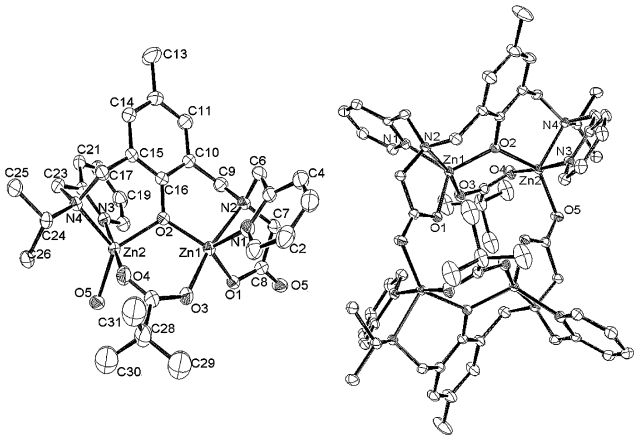

Fig. 2 An ORTEP representation of the structure of **3**, showing both the simpler dimer within the structure (left) and the complete dimer of dimers (right). Thermal ellipsoids are drawn at the 50% probability level for the simple dimer and at 30% for the dimer of dimers. Hydrogen atoms, non-coordinated counter ions and solvent molecules have been omitted for clarity. Relevant distances (Å) and angles (°): Zn(1)–O(2) 1.956(3); Zn(1)–O(3) 2.006(3); Zn(1)–O(1) 2.022(3); Zn(1)–N(1) 2.087(3); Zn(1)–N(2) 2.221(3); Zn(2)–O(5) 1.990(3); Zn(2)–O(2) 2.004(2); Zn(2)–O(4) 2.069(3); Zn(2)–N(4) 2.102(3); Zn(2)–N(3) 2.147(3); Zn(1)–O(2)–Zn(2) 118.02(13); O(3)–Zn(1)–N(2) 168.96(11); O(2)–Zn(1)–N(1) 122.24(12); O(4)–Zn(2)–N(3) 175.98(12); O(5)–Zn(2)–O(2) 138.36(11).

complexes (3.35–3.40 Å).[20] The two zinc ions are in octahedral N_2O_4 environments and the two exogenouscarboxylates bridge unsymmetrically with their shortest O–M bonds being *trans* to the tertiary amines and their longer bonds *trans* to the pyridyls. The phenoxide bridge is symmetric with the two Zn–$O_{phenolate}$ distances differing by approx. 0.005 Å and both bonds being *trans* to the terminal carboxylates.

Complexes **2** and **3** are isostructural in the solid state. The discussion below is restricted to the structure of **3** while relevant data for the structure of **2** are presented in the ESI.§ The molecular structure of the cation of **3** (Fig. 2) reveals that the dizinc complex crystallizes as a dimer of dimers, where the two phenolate-bridged dinuclear entities are linked by the terminal carboxylates of the two IPCPMP ligands, each of which bridges two zinc ions that belong to different dimers, by *syn*,*anti*-coordination. There is thus an overall inversion center. The separation between the zinc ions is significantly shorter (3.40 Å) than in **1**. As in **1**, the pyridyl groups are in relative *trans* positions to each other. Both zinc ions are five-coordinate, being coordinated by N_2O_3 donor sets in distorted trigonal bipyramidal geometries with τ values[21] of 0.78 for Zn1 and 0.63 for Zn2. The phenolate moiety coordinates in an equatorial position on both zinc ions and forms a slightly unsymmetrical bridge (ΔZn–$O_{phenolate}$ approx. 0.05 Å). The FAB mass spectrum of **3** reveals a major cluster of peaks at 675 amu with an isotope pattern corresponding to the dinuclear "monomer" $[Zn_2IPCPMP\{O_2CC(CH_3)_3\}]^+$ and a minor cluster of peaks at 1495 that can be fitted to the dimer of dimers plus one hexafluorophosphate anion. The corresponding mass spectrum of the complex in an MeCN–H_2O solution (1 : 1 v/v), which is the solvent mixture that was used in kinetic investigations (*vide infra*), displays the peak at 675 amu while no peaks corresponding to the dimer of dimers can be detected, suggesting that **3** dissociates into two dinuclear complexes in this solvent mixture. The FAB mass spectra of a solid state sample of **2**, and of **2** in a 1 : 1 v/v MeCN–H_2O solution, exhibit major peaks at 633 amu corresponding to the dinuclear complex $[Zn_2IPCPMP(O_2CCH_3)]^+$. In addition, a minor peak ascribable to $[\{Zn_2IPCPMP(O_2CCH_3)\}_2]^{2+}PF_6^-$ (1411 amu, relative intensity 2.5%) was found in the FAB (but not in the electrospray) mass spectrum of the solution sample (*cf*. ESI§). An identical mass spectrum was obtained when **2** was prepared *in situ*, but the peak attributed to the tetranuclear species disappears on prolonged standing in solution. The results suggest a relatively slow dissociation of the tetranuclear complex to form the corresponding dinuclear complex.

The coordination of the carboxylate groups may be studied by IR spectroscopy,[17,22] with unidentate, bridging and chelating coordination modes being distinguished by the separation of the ν_s and ν_{as} resonances, as well as their absolute positions. In the solid state (KBr pellet) IR spectrum of **1**, in which the "terminal" carboxylates actually bridge Zn and Na ions, there is no large separation between the major ν_s and ν_{as} resonances. For **3** the presence of only one set of carboxylate-derived peaks and the absence of a large separation is explained by the bridging coordination of both the endogenous and exogenous carboxylates. The solid state IR spectrum of **2** resembles that of **3**, with relatively stronger ν_{as} resonances.

The catalysis of HPNP (2-hydroxypropyl-*p*-nitrophenyl phosphate)[23] hydrolysis/transesterification by **1** and **2** was studied using *in situ* prepared complexes in buffered MeCN–H_2O (1 : 1) solutions at 25 °C and at pH 7–10.§§ The observed rate constants were determined using the initial rate method monitoring the formation of 4-nitrophenolate by measuring its absorbance at 400 nm ($\varepsilon = 18\,500$ M^{-1} cm^{-1}), taking into account

its acid dissociation constant ($pK_a = 7.15$) using the Henderson–Hasselbalch equation.[24] For comparison, the rate acceleration of HPNP hydrolysis by "free" $Zn(OAc)_2$ was also studied. The results are shown in Fig. 3. The observed rate constants for HPNP transesterification by the complexes in this study are on the same order of magnitude as some previous systems studied under similar conditions.[17,24–26] The complex with the asymmetric ligand has a considerably higher observed rate constant than the complex with the symmetric ligand. The asymmetric complex also yields higher rates than the reference reaction with $Zn(OAc)_2$ at equal total concentrations of zinc ions. On the other hand, the symmetric complex shows less activity than $Zn(OAc)_2$ below pH 8.5 but higher above, due to precipitation of zinc hydroxide from $Zn(OAc)_2$ solutions at high pH. The asymmetric complex shows activity at low pH (< 8) in contrast to the other catalysts and the uncatalyzed reaction. The transesterification of the HPNP substrate may be initiated *via* deprotonation of the substrate by a free or metal-bound hydroxyl moiety,[27,28] and it is likely that the reason for the higher initial rates observed for the asymmetric complex is due to the available coordination site in this complex, which facilitates the binding and deprotonation of water, although enhancement of the catalysis by the presence of the (coordinatively unsaturated) tetranuclear complex can not be ruled out (*vide supra*). Current studies are directed toward further elucidation of the observed difference in catalytic activity and the possible effect that the different electronic influences of the ligand environment on the reactivities for the two types of complexes.

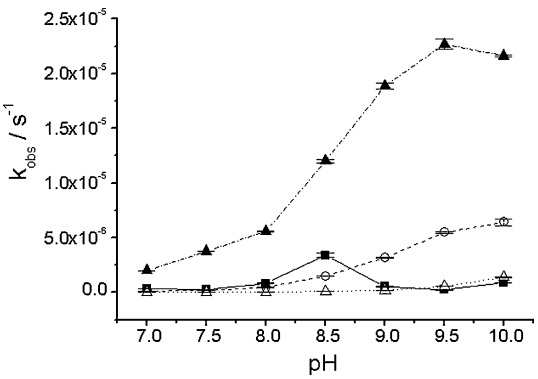

Fig. 3 A plot of k_{obs} *vs.* pH for the hydrolysis/transesterification of HPNP by complexes **1** and **2** as well as $Zn(OAc)_2$ in buffered H_2O–MeCN (1 : 1, v/v) solution at 25 °C. --- ▲--- H_4IPCPMP$(PF_6)_2$ + $2Zn(OAc)_2$; ---○--- Na_3BCPMP + $2Zn(OAc)_2$; –■– $Zn(OAc)_2$; · · · △ · · · uncatalyzed.

We would like to thank the Swedish Research Council (VR) for financial support and Dr Einar Nilsson for help with the measurement of mass spectra. This research has been carried out within the framework of the International Research Training Group *Metal Sites in Biomolecules: Structures, Regulation and Mechanisms* (www.biometals.eu).

Notes and references

* Analytical data: H_4IPCPMP$(PF_6)_2 \cdot H_2O$ Elem. Anal. Calc. $C_{26}H_{36}F_{12}N_4O_4P_2$: C, 41.17; H, 4.78; F, 30.06; N, 7.39; Found: C, 41.2; H, 4.8; F, 29.9; N, 7.2; IR (KBr)/cm^{-1}: 1710(s, C=O of $–CO_2H$); 1615(m), 1540(w), 1490(m, aromatic C=C); 1241(m, C–OH of $–CO_2H$); 1227(m); 844(s) (aromatic C–H bending); 558(s); UV/vis (acetonitrile)/nm: 220(sh); 260; 287; ^{1}H-NMR (500 MHz) CD_3CN δ 8.48 (d, 1H, ^3J = 5.8 Hz), 8.46 (d, 1H, ^3J = 4.8 Hz), 8.25 (t, 1H, ^3J = 7.9 Hz), 7.78 (t, 1H, ^3J = 7.8 Hz), 7.73 (t, 1H, ^3J = 6.8 Hz), 7.61 (d, 1H, ^3J = 8.0 Hz), 7.34 (dd, 1H, ^3J = 5.3 Hz, ^3J = 7.1 Hz), 7.25 (d, 1H, ^3J = 7.8 Hz), 6.93 (s, 2H), 4.35 (s, 2H, br), 4.18 (s, 2H, br), 4.09 (s, 2H), 3.83 (s, 2H), 3.69 (s, 2H), 3.68 (sept, 1H, ^3J = 6.6 Hz), 2.14 (s, 3H), 1.44 (d, 6H, ^3J = 6.6 Hz).
Na_3BCPMP·4NaOH Elem. Anal. Calc. $C_{25}H_{29}N_4Na_7O_9$: C, 43.49; H, 4.23; N, 8.11; Found: C, 44.029; H, 3.814; N, 8.133; IR (KBr) cm^{-1}: 1586(s, $–CO_2^-$ asym.); 1471(m, aromatic C–C); 1442(m); 1412(m, $–CO_2^-$ sym.); 1331(m); 866(w, aromatic C–H bend); 767(m, aromatic C–H bend); ^{1}H-NMR (500 MHz) CD_3OD δ 2.15 (s, 3 H), 3.07 (s, 4 H), 3.56 (m, 4H), 3.65 (m, 4 H), 6.77 (s, 2 H), 7.19 (t, ^3J = 6.3 Hz, 2 H), 7.26 (d, ^3J = 8 Hz, 2 H), 7.64 (dt, ^3J = 7.5 Hz, 2 H), 8.47 (d, ^3J = 5 Hz, 2 H).
†† **1**: $Na_3[Zn_2(BCPMP)(OAc)_2]_2PF_6 \cdot 6H_2O$ Elem. Anal. Calc. $C_{58}H_{74}F_6N_8Na_3O_{24}PZn_4$: C, 39.97; H, 4.28; N, 6.43; Found C, 40.2; H, 4.4; N, 6.5; IR (KBr)/cm^{-1}: 2920(w); 1601(s, asym. $–CO_2$); 1590(s); 1477(m); 1418(m, sym. $–CO_2$); 1397(m, sym. $–CO_2$); 838(s); UV/Vis (acetonitrile)/nm: 234(sh); 260; 298; FAB+ MS: m/z (^{64}Zn) 753 ($[Zn_2(BCPMP)(OAc)_2]^-$ + $2Na^+$); 671 ($[Zn_2(BCPMP)(OAc)] + Na^+$); 589 ($[Zn_2(BCPMP)]^+$;
2: $[\{Zn_2(IPCPMP)(OAc)\}_2](PF_6)_2$ Elem. Anal. Calc. $C_{56}H_{66}F_{12}N_8O_{10}P_2Zn_4$: C, 43.04; H, 4.26; N, 7.17; Found C, 42.8; H 4.4; N, 7.0 IR (KBr)/cm^{-1}: 2964(w); 2921(w); 1609(s, asym. $–CO_2$); 1598(s, asym. $–CO_2$); 1562(m); 1486(m); 1435(m, sym. $–CO_2$); 1414(m, sym. $–CO_2$); 844(s); 559(m); UV/vis (acetonitrile)/nm: 234(sh); 260; 298; FAB+ MS: m/z (^{64}Zn) 829 ($[Zn_2(IPCPMP)(OAc)_2] + NB^+$, NB^+ = 3-nitrobenzyl cation, matrix); 633 ($[Zn_2(IPCPMP)(OAc)]^+$); 619 ($[Zn_2(IPCPMP)(O_2CH)]^+$); 591 ($[Zn_2(IPCPMP)(OH)]^+$); 1411 ($[\{Zn_2(IPCPMP)(O_2CCH_3)\}_2]^{2+} \cdot PF_6^-$);
3: $[\{Zn_2(IPCPMP)(O_2CC(CH_3)_3\}_2](PF_6)_2 \cdot 2H_2O \cdot 2C_2H_5OH$ Elem. Anal. Calc. $C_{64}H_{86}F_{12}N_8O_{12}P_2Zn_4$: C, 44.93; H, 5.07; N, 6.55; Found C, 44.5; H, 5.1; N, 6.4; IR (KBr)/cm^{-1}: 2970(w); 2921(w); 2871(w); 1609(s, asym. $–CO_2$); 1562(m); 1482(m); 1442(w); 1418(m); 844(s); 553(m); UV/Vis (acetonitrile)/nm: 233(sh); 261; 298; FAB+ MS: m/z (^{64}Zn) 675 ($[Zn_2(IPCPMP)(O_2CC(CH_3)_3]^+$); 1495 ($[\{Zn_2(IPCPMP)(O_2CC(CH_3)_3)\}_2]^{2+} PF_6^-$)
‡‡ Diffraction data was collected at 120 K on a Bruker AXS BV CCD diffractometer. The structures were solved using direct methods (SHELXS) and refined by full-matrix least squares against F^2. **1**: $Na_3[Zn_2(BCPMP)(OAc)_2]_2PF_6 \cdot 6H_2O$; The Na2, O13, and O14 atoms are disordered over two sites with equal occupancies. All hydrogens connected to the Na bound oxygens have been omitted. Other hydrogen atoms were positioned geometrically and were also constrained to ride on their parent atoms. $C_{58}H_{66}F_6N_8Na_3O_{24}PZn_4$, M = 1734.61, monoclinic, $P2_1/c$, a = 19.5230(5) Å, b = 10.1399(2) Å, c = 18.1745(5) Å, β = 90.181(3)°, V = 3597.83(15) Å^3, Z = 2, T = 120(2)K, data/restraints/parameters 7067/12/487, R(int) = 0.0367, $R1$ = 0.0653, $wR2$ = 0.1736 (observed data).
3: $[Zn_2(IPCPMP)(O_2CC(CH_3)_3]PF_6H_2O \cdot C_2H_5OH$ The idealized positions of the H_2O hydrogens were estimated with HYDROGEN (Nardelli, 1999) program and constrained to ride on their parent atom. These hydrogen atoms were disordered over two sites with equal occupancies. The OH hydrogen atom was located from the difference Fourier map but constrained to ride on its parent atom. Other hydrogen atoms were positioned geometrically and also constrained to ride on their parent atoms. Hydrogen atoms were positioned geometrically and refined using the riding model. $C_{64}H_{86}F_{12}N_8O_{12}P_2Zn_4$, M = 1710.83, monoclinic $C2/c$, a = 24.5080(5) Å, b = 14.4476(3) Å, c = 21.2277(3) Å, β = 93.3150(10)°, V = 7503.8(2) Å^3, Z = 4, T = 120(2)K, data/restraints/parameters = 8289/29/479, R(int) = 0.375, $R1$ = 0.0453, $wR2$ = 0.1145 (observed data). See ESI§ for crystallographic details for **2**. CCDC reference numbers 659750, 659751 and 667079. For crystallographic data in CIF or other electronic format see DOI: 10.1039/b713664a
§§ Ionic strength and pH were kept constant by using total concentrations of 0.1 M of $NaClO_4$ and 0.01 M buffer (pH 7.0–7.5 MOPS, pH 8.0–8.5 TRIS, pH 9.0–9.5, pH 10.0 CAPS).

1 D. Kopp and S. J. Lippard, *Curr. Opin. Chem. Biol.*, 2002, **6**, 568–567.
2 M. Baik, M. Newcomb, R. A. Friesner and S. J. Lippard, *Chem. Rev.*, 2003, **103**, 2385–2419.
3 H. Decker, T. Schweikardt and F. Tuczek, *Angew. Chem., Int. Ed.*, 2006, **45**, 4546–4550.
4 E. I. Solomon, U. M. Sundaram and T. E. Machonkin, *Chem. Rev.*, 1996, **96**, 2563–2605.
5 N. Mitic, S. J. Smith, A. Neves, L. W. Guddat, L. R. Gahan and G. Schenk, *Chem. Rev.*, 2006, **106**, 3338–3363.
6 S. Ciurli, S. Benini, W. R. Rypniewski, K. S. Wilson, S. Miletti and S. Mangani, *Coord. Chem. Rev.*, 1999, **190–192**, 331–355.

7 J. A. Cricco, E. G. Orellano, R. M. Rasia, E. A. Ceccarelli and A. J. Vila, *Coord. Chem. Rev.*, 1999, **190–192**, 519–535.
8 W. N. Lipscomb and N. Sträter, *Chem. Rev.*, 1996, **96**, 2375–2433.
9 J. Weston, *Chem. Rev.*, 2005, **105**, 2151–2174.
10 M. Matsui, J. H. Fowler and L. L. Walling, *Biol. Chem.*, 2006, **387**, 1535–1544.
11 A. Volbeda, A. Lahm, F. Sakiyama and D. Suck, *EMBO J.*, 1991, **10**, 1607.
12 M. B. Twitchett and A. G. Sykes, *Eur. J. Inorg. Chem.*, 1999, 2105–2115.
13 E. E. Kim and H. W. Wyckoff, *J. Mol. Biol.*, 1991, **218**, 449–464.
14 U. Heinz and H.-W. Adolph, *Cell. Mol. Life Sci.*, 2004, **61**, 2827–2839.
15 H. Carlsson, M. Haukka and E. Nordlander, *Inorg. Chem.*, 2002, **41**, 4981–4983.
16 H. Carlsson, M. Haukka, A. Bousseksou, J. Latour and E. Nordlander, *Inorg. Chem.*, 2004, **43**, 8252–8262.
17 H. Carlsson, M. Haukka and E. Nordlander, *Inorg. Chem.*, 2004, **43**, 5681–5687.
18 E. Lambert, B. Chabut, S. Chardon-Noblat, A. Deronzier, G. Chottard, A. Bousseksou, J. Tuchagues, J. Laugier, M. Bardet and J. Latour, *J. Am. Chem. Soc.*, 1997, **119**, 9424–9437.
19 M. M. Benning, S. B. Hong, F. M. Raushel and H. M. Holden, *J. Biol. Chem.*, 2000, **275**, 30556–30560.
20 H. Adams, D. Bradshaw and D. E. Fenton, *Inorg. Chim. Acta*, 2002, **332**, 195–200.
21 The structural index τ is defined as $\tau = (\beta - \alpha)/60°$, where α and β are the two largest angles around the metal: A. W. Addison, T. N. Rao, J. Reedijk, J. van Rijn and G. C. Verschoor, *J. Chem. Soc., Dalton Trans.*, 1984, 1349.
22 G. B. Deacon and R. J. Phillips, *Coord. Chem. Rev.*, 1980, **33**, 227–250.
23 HPNP = 2-hydroxypropyl-*p*-nitrophenyl phosphate barium salt, synthesized according to: D. M. Brown and D. A. Usher, *J. Chem. Soc.*, 1965, 6558–6565.
24 S. Albedyhl, M. T. Averbuch-Pouchot, C. Belle, B. Krebs, J. L. Pierre, E. Saint-Aman and S. Torelli, *Eur. J. Inorg. Chem.*, 2001, 1457–1464.
25 S. Albedyhl, D. Schnieders, A. Jancsó, T. Gajda and B. Krebs, *Eur. J. Inorg. Chem.*, 2002, 1400–1409.
26 C. He and S. J. Lippard, *J. Am. Chem. Soc.*, 2000, **122**, 184–185.
27 L. Bonfa, M. Gatos, F. Mancin, P. Tecilla and U. Tonellato, *Inorg. Chem.*, 2003, **42**, 7737.
28 F. Mancin and P. Tecilla, *New J. Chem.*, 2007, **31**, 800–817.
29 ORTEP-3 for Windows:L. J. Farrugia, *J. Appl. Crystallogr.*, 1997, **30**, 565(http://www.chem.gla.ac.uk/~louis/software/ortep3/).